

## Levels of $^{64}\text{Ga}$ via the $^{64}\text{Zn}(p, n)$ and $^{64}\text{Zn}(p, n\gamma)$ reactions\*

L. F. Hansen, J. C. Davis, F. S. Dietrich, M. C. Gregory, and R. P. Koopman

Lawrence Livermore Laboratory, Livermore, California 94550

(Received 1 April 1974)

The  $(p, n)$  and  $(p, n\gamma)$  reaction in  $^{64}\text{Zn}$  has been studied from 8.0 up to 10.5 MeV in order to obtain the level structure of  $^{64}\text{Ga}$ . The threshold of the  $(p, n)$  reaction obtained from an excitation function of the  $\gamma$  rays gave a  $Q$  value of  $-7.968 \pm 0.020$  MeV. The measured angular distribution of the neutrons and their cross sections at 10 and 10.5 MeV were compared with the predictions of a Hauser-Feshbach calculation. These results plus the measurements of the cascade  $\gamma$  rays among the levels and the lifetimes of some of them allowed the assignment of spins for some of the low excited levels in  $^{64}\text{Ga}$ .

NUCLEAR REACTIONS  $^{64}\text{Zn}(p, n)$ ,  $(p, n\gamma)$ .  $E = 8.0\text{--}10.5$  MeV; measured  $\sigma_n(E, \theta)$ ,  $\sigma_\gamma(E, \theta = 90^\circ)$ ,  $\gamma$  lifetimes. Hauser-Feshbach analysis.  $^{64}\text{Ga}$  levels, deduced  $J, \pi$ .

### INTRODUCTION

The interest in the level structure of  $^{64}\text{Ga}$  has been motivated as a result of the experimental evidence<sup>1,2</sup> for the existence of  $^{64}\text{Ge}$ . This nucleus has been predicted to be particle stable,<sup>3</sup> and calculations by Arnett, Truran, and Woosley<sup>4</sup> have shown that  $^{64}\text{Ge}$  is an " $\alpha$ -particle" nucleus ( $N = Z = 32$ ), whose abundance could be explained as the result of being formed during explosive nucleosynthesis at high temperatures.  $^{64}\text{Ge}$  will  $\beta$  decay by positron emission to excited levels of  $^{64}\text{Ga}$ , which are assumed to be  $1^+$  levels if the ground state of  $^{64}\text{Ge}$  is a  $0^+$ . In turn  $^{64}\text{Ga}$  will  $\beta$  decay to  $^{64}\text{Zn}$ . The chain  $^{64}\text{Ge} \rightarrow \beta \text{ decay} \rightarrow ^{64}\text{Ga} \rightarrow \beta \text{ decay} \rightarrow ^{64}\text{Zn}$  would then account for the abundance<sup>4</sup> of this last isotope in nature. In the present work the  $^{64}\text{Zn}(p, n)^{64}\text{Ga}$  and  $^{64}\text{Zn}(p, n\gamma)^{64}\text{Ga}$  reactions have been studied to obtain information on the level structure and spin assignments of the levels in  $^{64}\text{Ga}$ . The measured angular distributions of the neutrons and their cross sections for 10.0- and 10.5-MeV incident proton energy were compared with the predictions of a Hauser-Feshbach calculation.<sup>5</sup> These results plus measurements of the cascade  $\gamma$  rays among the levels, their angular distributions, and the lifetimes of some of them allowed the assignment of spins for some of the low excited levels in  $^{64}\text{Ga}$ .

The threshold of the  $(p, n)$  reaction in  $^{64}\text{Zn}$  was obtained from an excitation function of the  $\gamma$  rays observed between 8.0 and 10.0 MeV. These measurements gave a  $Q$  value of  $-7.968 \pm 0.020$  MeV. This value compares with  $-7.854 \pm 0.03$  MeV quoted in the 1971 mass evaluation,<sup>6</sup>  $-7.953 \pm 0.006$  MeV, and  $-7.963 \pm 0.010$  MeV reported by Davids, Matthews, and Whitmire<sup>7</sup> and Robertson,<sup>8</sup> respectively. Our value yields a mass excess (using Ref. 6) of  $-58.821 \pm 0.020$  MeV.

### EXPERIMENTAL METHOD

#### Energy measurements

Protons with energies between 8.0 and 10.5 MeV were produced by the Livermore EN tandem Van de Graaff. The targets were self-supporting foils 99.66%  $^{64}\text{Zn}$  enriched isotope with thicknesses of 2.0 and 0.81 mg/cm<sup>2</sup>. The thicker target was used for the  $\gamma$  measurements, while the thinner one was used in the neutron measurements. The neutrons were detected with 16 NE 213 liquid scintillation detectors located between 3.5 and 159°. (The experimental arrangement and electronics of the neutron time-of-flight facilities at Livermore have been described in detail elsewhere.)<sup>9</sup> The neutron energies, in the range between 1 and 2 MeV, were determined by time of flight over a 10.8 m flight path. To permit identification of the low excited states of  $^{64}\text{Ga}$ , where the separation between some levels is less than 50 keV, low neutron energies (1–2 MeV) were necessary to achieve sufficient separation between the neutron peaks. Detection of neutrons with energies below 1 MeV was not reliable because of the large uncertainties in the detector efficiency at these low energies. The detectors were set for a lower bias of 1 MeV which corresponds to half the pulse height of the Compton edge of the 0.511-MeV  $\gamma$  ray from a  $^{22}\text{Na}$  source. Pulse shape discrimination was used to minimize the  $\gamma$  background. The neutron spectrum taken at 10.5 MeV is shown in Fig. 1. At lower proton energies the separation between the g.s., 43-, 128-, 172-, and 322-keV levels was greater because of the lower energy of the neutrons. The neutron spectra from 9.0- and 9.5-MeV protons were used to obtain the excitation energies of the levels excited by neutron emission.

The  $\gamma$  rays with energies between 20 keV and 4.0

MeV were detected with an 8 cm<sup>3</sup> Ge(Li) detector with a resolution of 1.03 keV for <sup>57</sup>Co and 2.26 keV for <sup>60</sup>Co. For proton energies between 8 and 10 MeV, all the  $\gamma$  rays with energies above 800 keV were associated with the ( $p, p'\gamma$ ) reactions in <sup>64</sup>Zn.

The scattering chamber was a rectangular stainless steel box 17.6 cm wide and 6.625 cm high. The  $\gamma$  rays were observed through a 0.025 cm thick Mylar window, 43.50 cm long and 3.81 cm wide along the side of the chamber. This window allows angular distribution measurements between 20 and 160°. A Faraday cup 3 m away from the chamber was used to monitor the beam; it was shielded by a large cylinder 40.64 cm thick, 76.20 cm long with a 20.32 cm hole through the center to allow the beam pipe to go through. This cylinder was filled with a mixture of amorphous boron and paraffin, 30 and 70% by weight, respectively. The end of the cylinder facing the detector was covered by 10 cm of lead. This shielding was very effective in reducing the  $\gamma$ -ray background from the Faraday cup. The only  $\gamma$ -ray peaks observed in the background runs were 0.511 MeV and the x rays from the lead shielding around the detector,

which was a cylinder 1.83 cm thick and 15 cm long with a 2.54 cm hole at the face of the detector. In later runs these x rays were eliminated by surrounding the detector with a graded shield made of concentric cylinders of Pb, Ta, Sn, and Cu, 1.91, 0.01, 0.08, and 0.05 cm thick, respectively. An 0.05 cm Al absorber was set at the face of the detector to absorb the x rays from the <sup>64</sup>Zn target (about 98% absorption for 10-keV  $\gamma$  ray), allowing maximization of the ratio of peak to background for the low energy  $\gamma$  rays from <sup>64</sup>Ga.

The electronics used with the Ge(Li) detector was a high counting rate system designed by Goulding, Landis, and Pehl.<sup>10</sup> This system was able to handle up to  $5 \times 10^4$  pulses per sec.

The  $\gamma$ -ray spectra were taken for two energy intervals: (1) a low energy (LE) interval from a few keV up to 600 keV, and (2) a high energy (HE) interval from a few keV up to 4 MeV. The first interval allowed better separation between the peaks. All spectra were taken in a 4096 channel analyzer. The energy calibrations were done using calibrated energy sources (<sup>241</sup>Am, <sup>57</sup>Co, <sup>203</sup>Hg, <sup>113</sup>Sn, <sup>22</sup>Na, <sup>137</sup>Cs, <sup>54</sup>Mn, <sup>60</sup>Co, and <sup>88</sup>Y) whose

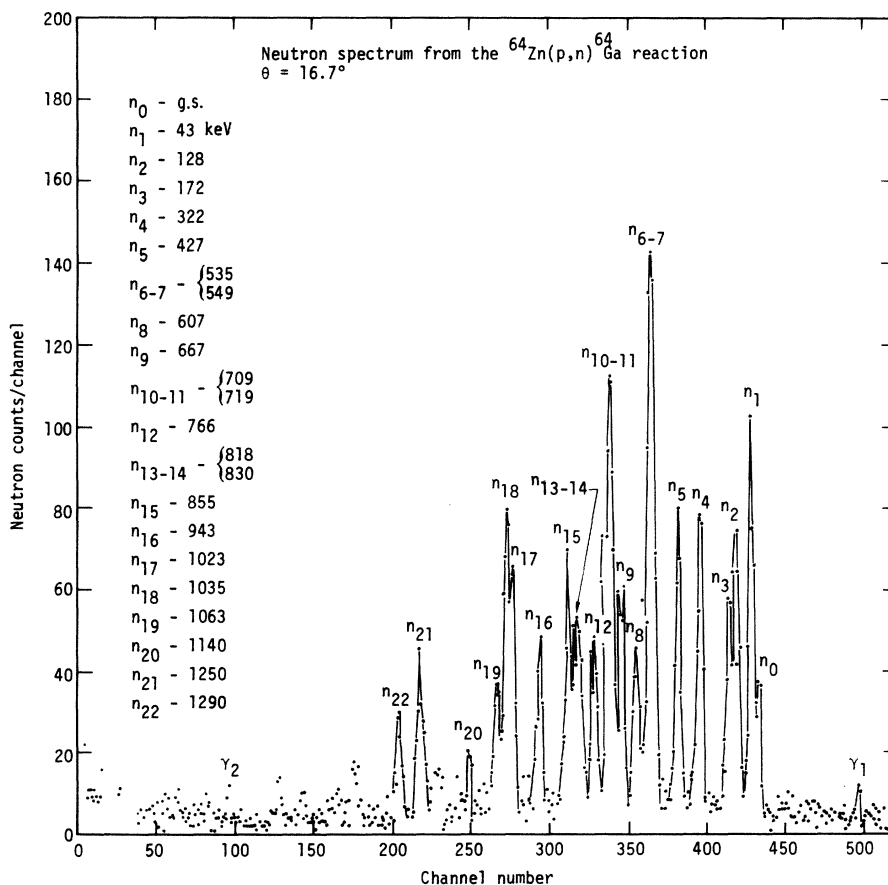


FIG. 1. Neutron spectrum from the <sup>64</sup>Zn( $p, n$ )<sup>64</sup>Ga reaction from 10.5-MeV protons.

characteristic  $\gamma$  rays were observed simultaneously with the  $\gamma$  rays from the  $^{64}(p, n\gamma)^{64}\text{Ga}$  reaction. The calibration was obtained from a polynomial fit, where the number of counts at a given energy was weighted by the statistical error and the error in the energy source. The unknown energies were then calculated using the entire covariant matrix at the 95% confidence level. The efficiency of the detector as a function of  $\gamma$ -ray energy was determined by positioning the calibrated sources at the target holder in the scattering chamber, to assure that the corrections for absorption and solid angle were properly handled. The energy calibration of the system for the high energy measurements was determined by fitting the  $\gamma$  spectrum from a  $^{56}\text{Co}$  source, in addition to the sources listed above. The values of the  $\gamma$ -ray energies for this source were those reported by Camp and Meredith.<sup>11</sup> In Figs. 2 and 3 are shown the spectra for the LE and HE intervals. The  $^{64}\text{Zn}$  target, 99.66% enriched, had a 0.21%  $^{66}\text{Zn}$  contamination. At proton energies close to the threshold of the  $(p, n)$  reaction in  $^{64}\text{Zn}$ , the presence of a 43.8-keV  $\gamma$  ray from the  $^{66}\text{Zn}(p, n)^{66}\text{Ga}$  reaction made it difficult to measure the threshold of

the first excited state in  $^{64}\text{Ga}$  at 42.89 keV, as well as its lifetime. To separate these two  $\gamma$  rays, a Si(Li) detector was used.<sup>12</sup> The insert in Fig. 2 shows them clearly resolved. To confirm the identification of those  $\gamma$  rays associated with the  $(p, n\gamma)$  reaction, an excitation function was measured for proton energies between 8 and 10 MeV. The  $\gamma$  rays produced by the  $(p, p'\gamma)$  reaction in  $^{64}\text{Zn}$  were all present at the threshold of the  $(p, n)$  reaction and their excitation function was slowly varying at these energies. The activation spectrum from the  $\gamma$  decay of  $^{64}\text{Ga}$  levels to  $^{64}\text{Zn}$  levels was also recorded and is shown in Fig. 4.

#### Half-life measurements

For the half-life measurements, a 10-MeV proton beam from the tandem was chopped and bunched to produce 2 nsec wide pulses with 400 nsec separation between pulses. The fast signal from the detector amplifier was used as the start pulse for the time-to-amplitude converter (TAC) and a timing signal from the chopper was used as the stop pulse.

Timing curves for the 42.9-, 85.2-, and 128.1-

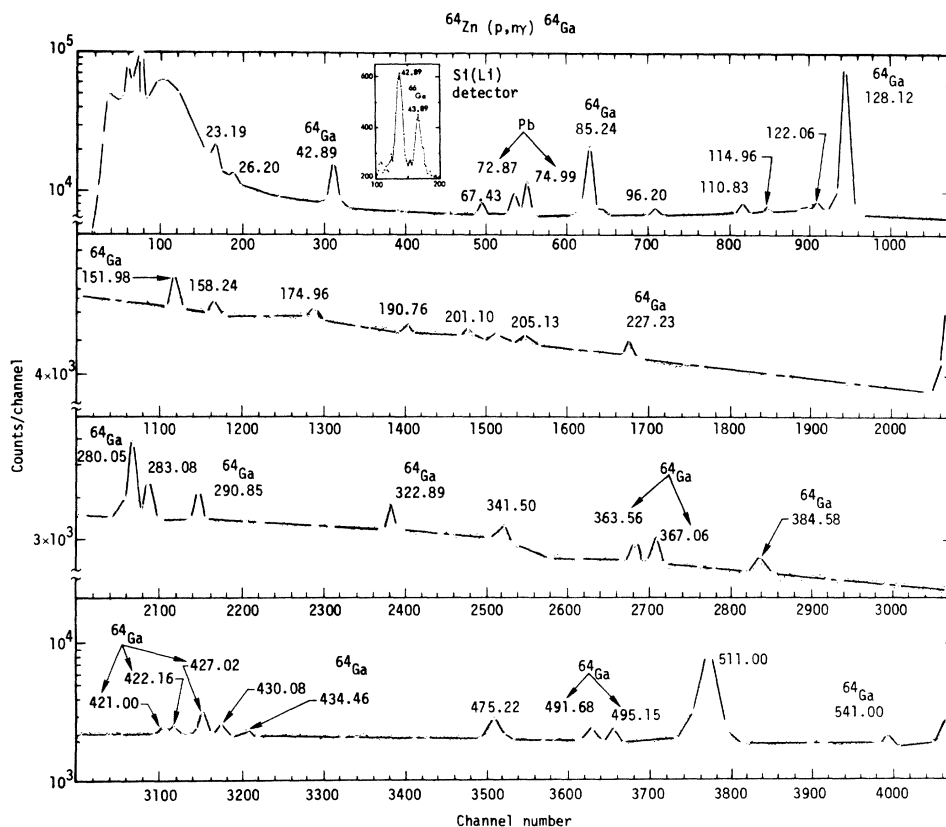


FIG. 2.  $\gamma$ -ray spectrum from the  $^{64}\text{Zn}(p, n\gamma)^{64}\text{Ga}$  reaction taken from a few keV up to 600 keV [low energy interval, (LE)] from 10.0-MeV protons.

keV  $\gamma$  rays were measured. In each case the TAC spectrum was gated by the energy spectrum with a window set to include only the  $\gamma$  ray in question. Background spectra, mainly due to Compton events from prompt  $\gamma$  rays of higher energy, were taken by setting energy windows just above or below the peak of interest. These spectra were subtracted from the spectra taken on the peaks after normalizing the background spectrum to the correct energy interval. For each  $\gamma$  ray of interest, the time response of the detector-electronic system to a known prompt radiation of about the same energy was measured using the same proton beam. The prompt radiations chosen were the 47.5-keV x ray from  $^{165}\text{Ho}$ , the 87.2-keV x ray from  $^{209}\text{Bi}$  and 136.2-keV  $\gamma$  ray from Coulomb excitation of  $^{181}\text{Ta}$ . A fitting function was made by assuming an exponential decay for the  $\gamma$  ray in question, and folding this decay curve with the corresponding measured prompt line shape. The lifetime and amplitude were then determined by least-squares fitting this function to the data. In Fig. 5 are shown the TAC spectra with background subtracted for the three  $\gamma$  transitions in  $^{64}\text{Ga}$ . The time spectrum shows that the 42-keV  $\gamma$  ray is delayed with a half-life,

$T_{1/2} > 1000$  nsec for this transition. The erratic behavior of the spectrum in the immediate vicinity of the prompt peak is due to the large background subtraction in this region. A search for a prompt component in this radiation is described below. The 85-keV  $\gamma$  ray exhibits a measurable lifetime. The average of three different measurements yields a value of  $T_{1/2} = 6.9 \pm 0.7$  nsec for this  $\gamma$  transition. An attempt to fit the 128-keV curve with a single lifetime is shown by the dashed curve in Fig. 5. However, the spectrum shows evidence for a second longer-lived component. Such a component can be expected, since the delayed 85-keV transition originates from a 128-keV level that may also decay to the ground state; a shorter-lived 128-keV transition then corresponds to the transition 171 keV  $\rightarrow$  43 keV. The solid curve shows a fit with two half-lives, in which one of the half-lives was fixed at 7.0 nsec. The remaining half-life and the intensities of the two components were varied to obtain the fit. In the case shown, the second half-life was 3.0 nsec. The value of the shorter half-life was not well determined because it is very sensitive to the background subtraction and the treatment of the prompt line shape.

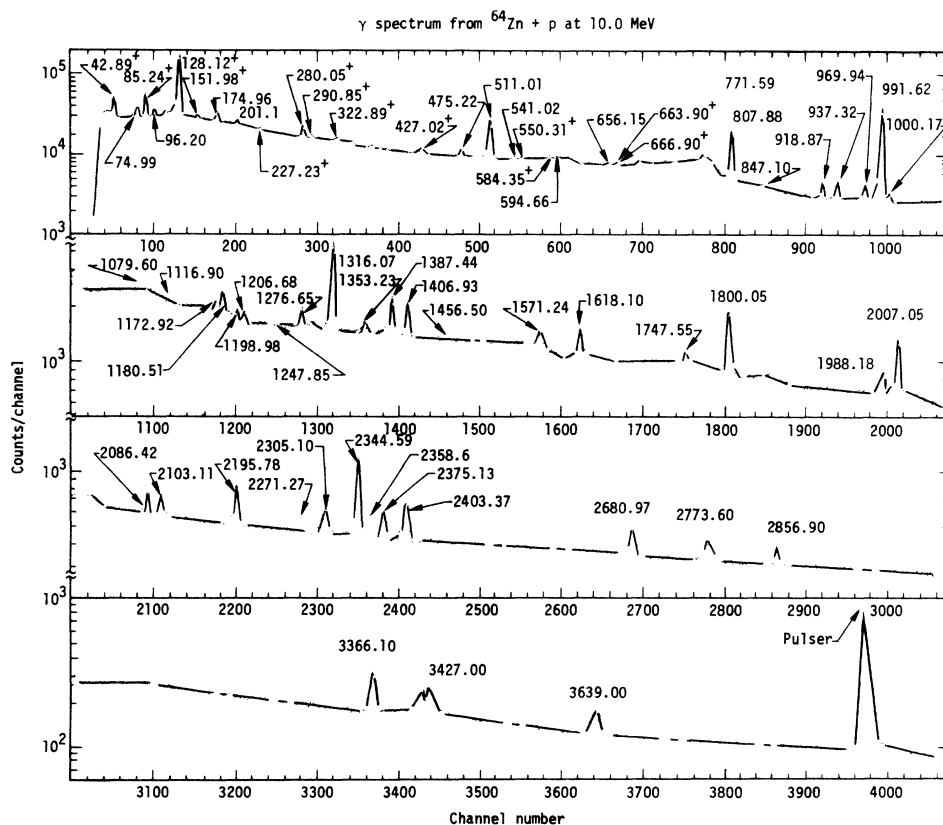


FIG. 3.  $\gamma$ -ray spectrum from the  $^{64}\text{Zn}(p, n)^{64}\text{Ga}$  reaction taken from a few keV up to 4 MeV [high energy interval, (HE)] from 10.0-MeV protons.

Although the TAC spectrum for the 42-keV  $\gamma$  ray shows that this radiation is predominantly delayed, the background subtraction in the prompt region is not accurate enough to eliminate the possibility of a prompt component. A search for a prompt component was carried out by observing the energy spectrum gated by time windows set on the TAC spectrum. The Si(Li) detector was used for these measurements, and the energy regions around the 85- and 128-keV radiations were investigated as well. The TAC output was sent to two single-channel analyzers. In the first one, a window was set to include the prompt peaks; in the other, the window covered a section of the flat part of the TAC spectrum corresponding to the delayed part of the spectrum. The widths of the prompt windows were 67.6 nsec for the 42.85-keV  $\gamma$  ray and 41.7 nsec for the 85- and 128-keV  $\gamma$  rays, respectively; the corresponding figures for the delayed windows were 387 and 470 nsec. The two windows were used to route the prompt and delayed energy spectra into different sections of the analyzer. These results are shown in Fig. 6, in

which the 42.89-keV radiation is seen in the delayed energy spectrum. The 67.4-keV  $\gamma$  ray could come from the  $^{66}\text{Zn}(p, n\gamma)^{66}\text{Ga}$  reaction or from the  $\beta$  decay of  $^{61}\text{Cu}$  from the  $^{64}\text{Zn}(p, \alpha)^{61}\text{Cu}$  reaction. In the prompt energy spectra are observed the 43.8-keV  $\gamma$  ray from  $^{66}\text{Ga}$  and the 85.2- and 128.1-keV  $\gamma$  rays from  $^{64}\text{Ga}$ . The small 42.89 peak seen in the prompt spectrum is entirely accounted for by the long half-life component seen in the delayed spectrum and in the TAC spectrum of Fig. 5. Normalizing prompt and delayed spectra by the ratio of the time window widths and subtracting leads to an upper limit of 3% for a prompt component in the 42-keV radiation.

#### ANALYSIS AND DISCUSSION OF THE RESULTS

##### Level scheme for $^{64}\text{Ga}$

From the  $\gamma$ -ray energies and the ordering of groups in the neutron spectra, the energy levels for  $^{64}\text{Ga}$  were deduced. They are listed in Table I. The energy levels  $n_8-n_7$ ,  $n_{10}-n_{11}$ ,  $n_{13}-n_{14}$ , and  $n_{16}-n_{17}$  were not completely resolved. Most of

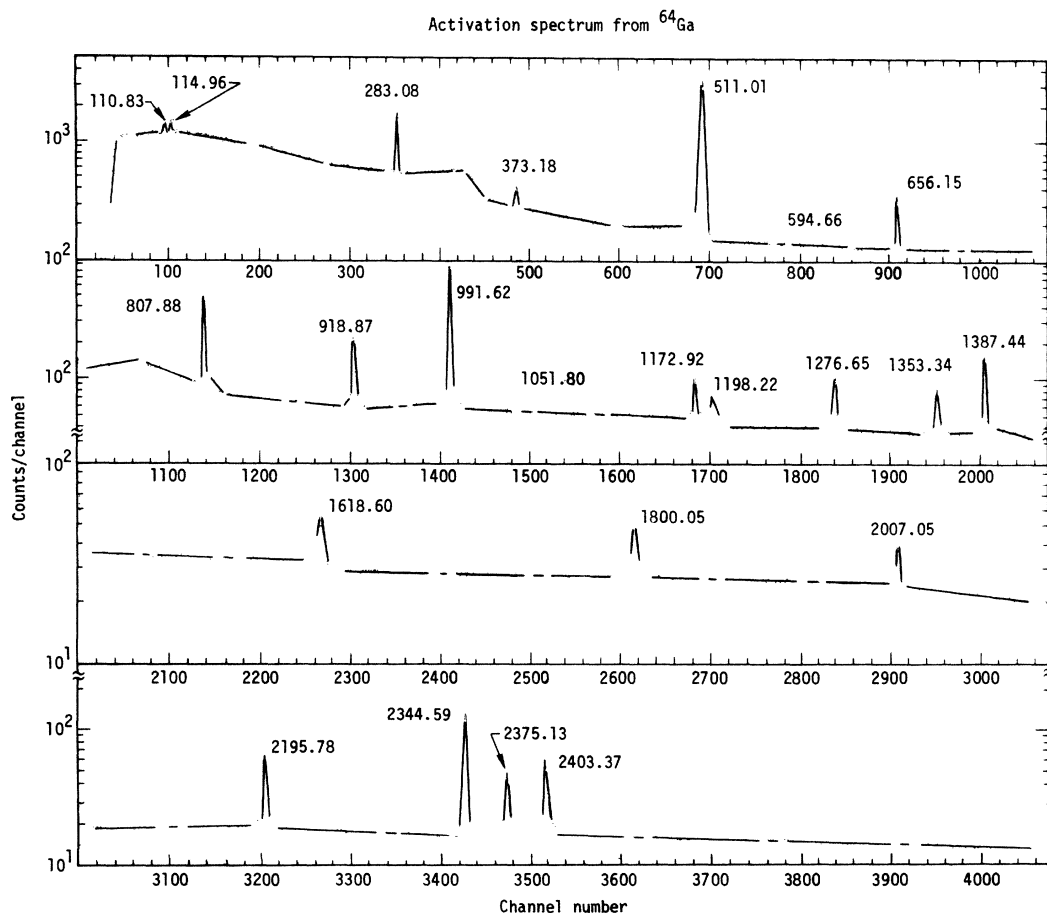


FIG. 4. Activation spectrum from the  $\beta$  decay of  $^{64}\text{Ga}$  levels to  $^{64}\text{Zn}$  levels.

these levels have been observed in the recent measurements of Robertson<sup>8</sup> for the  $^{64}\text{Zn}(^3\text{He}, t)^{64}\text{Ga}$  reaction. Preliminary results on these levels had also been published by King, Draper, and McDonald.<sup>13</sup> Three higher excitation levels at 1140, 1250, and 1290 keV were observed only at forward angles due to the bias cut of the detectors.

A Hauser-Feshbach calculation<sup>5</sup> was performed for 10.0- and 10.5-MeV proton bombarding energies. The transmission coefficients for the protons

and neutrons used in this calculation were obtained from an optical model calculation with the LOKI code<sup>14</sup>; one calculation was performed using Perey's optical parameters<sup>15</sup> for the protons, and for the neutrons the parameters given by Hodgson.<sup>16</sup> A second calculation was done taking Becchetti and Greenlees<sup>17</sup> optical parameters for protons and neutrons. Below 3 MeV, levels in  $^{64}\text{Zn}$  were taken from Ref. 18. Above 3 MeV, the levels were represented by a level density formula of the form

$$\rho(U, J) = K(2J+1)\exp[-J(J+1)/2\sigma^2]\exp(U/T), \quad (1)$$

where the values taken for the temperature  $T$  and spin cutoff parameter  $\sigma$  were 0.85 MeV and 3.4, respectively, and  $U$  is the excitation energy in the compound system. The normalization constant was obtained by equating the value for  $\rho$  at the neutron binding energy with that predicted by Gilbert and Cameron.<sup>19</sup>

The predicted cross sections for the two sets of optical parameters are compared with the measurements in Table II. The cross sections calculated with Becchetti and Greenlees<sup>17</sup> parameters are lower by 10 to 20% than those calculated with Perey<sup>15</sup> and Hodgson<sup>16</sup> optical parameters, and in better agreement with the measurements for the value of  $K$  chosen above. The accuracy of the Hauser-Feshbach calculation is not better than 30% because of uncertainties in the values of the transmission coefficients for the low excited states at energies close to the threshold of the  $(p, n)$

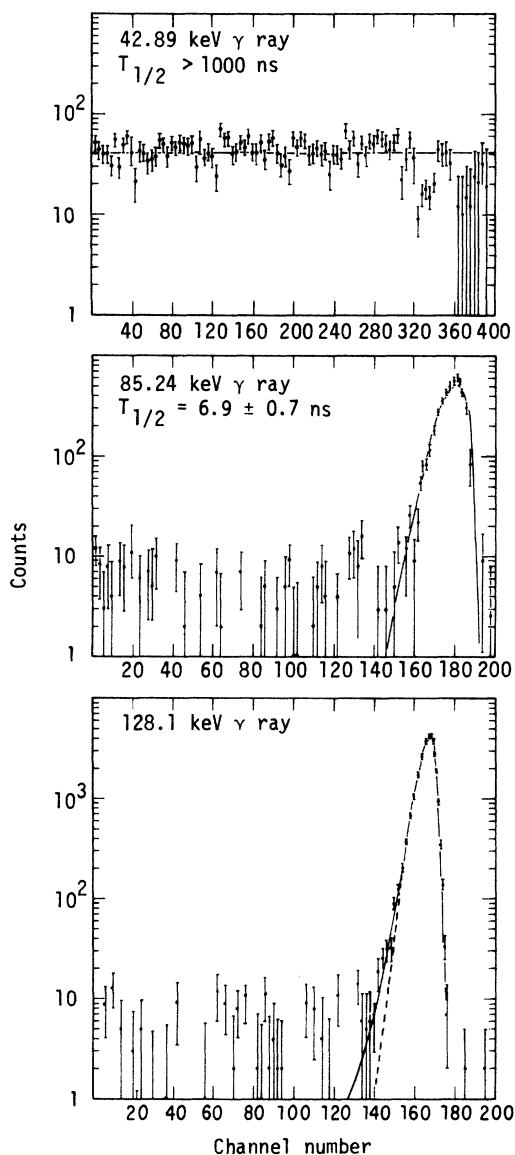


FIG. 5. TAC spectra with background subtracted for the three lower  $\gamma$  transitions in  $^{64}\text{Ga}$ . The solid curves are the best fit to the spectra. The difference between the solid and dashed line for the 128.1-keV  $\gamma$  ray is explained in the text. The time calibration is 1.8 nsec per channel; time increases from right to left with zero occurring at the peak location.

TABLE I. Energy levels for  $^{64}\text{Ga}$  deduced from the measurements of the  $^{64}\text{Zn}(p, n)^{64}\text{Ga}$  reaction.

Level	Excitation energy (keV)
$n_0$	g.s.
$n_1$	$43 \pm 2$
$n_2$	$128 \pm 3$
$n_3$	$172 \pm 3$
$n_4$	$322 \pm 3$
$n_5$	$427 \pm 4$
$n_6$	$535 \pm 5$
$n_7$	$549 \pm 5$
$n_8$	$607 \pm 5$
$n_9$	$667 \pm 6$
$n_{10}$	$709 \pm 5$
$n_{11}$	$719 \pm 5$
$n_{12}$	$766 \pm 7$
$n_{13}$	$818 \pm 5$
$n_{14}$	$830 \pm 8$
$n_{15}$	$855 \pm 8$
$n_{16}$	$943 \pm 5$
$n_{17}$	$1023 \pm 6$
$n_{18}$	$1035 \pm 6$
$n_{19}$	$1063 \pm 10$

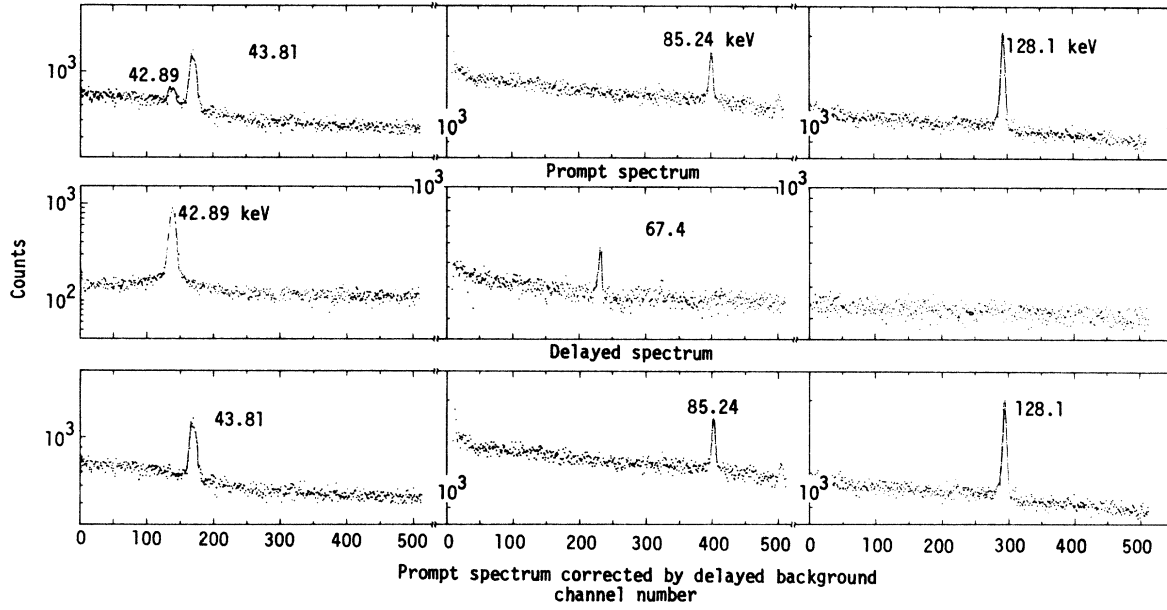


FIG. 6. Energy spectrum gated by time windows set on the TAC spectrum. In the upper and middle rows the windows were set to include the prompt + delayed and delayed part of the spectrum, respectively. In the lower row the delayed energy spectrum had been subtracted from the prompt + delayed spectrum after proper normalization.

TABLE II. Comparison between the measured neutron cross sections and the predicted values with a Hauser-Feshbach calculation for Perey-Hodgson optical parameters (Refs. 14 and 15) and Becchetti-Greenlees optical parameters (Ref. 16).

$E_p$ Level (MeV)	$\sigma(n)$ exp (mb)	$J^\pi$	$^{64}\text{Zn}(p, n)^{64}\text{Ga}$				
			10.0 MeV		10.5 MeV		
			$\sigma(n)$ (cal) (Refs. 14 and 15)	$\sigma(n)$ (cal) (Ref. 16)	$\sigma(n)$ exp (mb)	$\sigma(n)$ (cal) (Refs. 14 and 15)	$\sigma(n)$ (cal) (Ref. 16)
g.s.	$1.64 \pm 0.33$	$0^+$	2.99	2.32	$0.71 \pm 0.35$	1.82	1.39
0.043	$4.90 \pm 0.50$	$1^+$	6.01	5.38	$4.1 \pm 0.41$	4.31	3.45
		$2^+$	8.30	6.80		5.33	4.37
0.128	$2.71 \pm 0.54$	$1^+$	6.73	5.35	$2.39 \pm 0.48$	4.22	3.31
0.172	$5.20 \pm 0.52$	$2^+$	7.94	6.48	$3.47 \pm 0.35$	5.15	4.47
		$3^+$	6.58	5.77		4.50	3.93
		$3^-$	6.36	5.59		4.42	3.84
0.322	$5.40 \pm 0.54$	$2^+$	7.50	6.12	$3.80 \pm 0.38$	4.94	4.05
		$3^+$	6.17	5.42		4.29	3.64
		$3^-$	5.95	5.24		4.21	3.57
0.427	$2.56 \pm 0.50$	$1^+$	6.01	4.67	$3.13 \pm 0.31$	3.89	3.05
0.607	$3.30 \pm 0.66$	$2^+$	6.00	5.33	$2.83 \pm 0.56$	4.29	3.69
		$3^+$	5.23	4.64		3.85	3.34
		$3^-$	5.07	4.51		3.78	3.22
0.667	$2.40 \pm 0.50$	$1^+$	5.28	3.72	$2.48 \pm 0.50$	3.61	2.82
0.766	...	$2^+$			$3.06 \pm 0.31$	4.24	3.48
		$3^+$				3.61	2.96
		$3^-$				3.55	2.90
0.855	...	$1^+$	...	...	$3.41 \pm 0.34$	3.20	2.63
		$2^+$	...	...		4.08	3.35
0.943	...	$0^+$	...	...	$1.87 \pm 0.20$	1.38	1.06
		$1^+$	...	...		3.30	2.54

reaction (these values are sensitive to the optical parameters used in the calculation); and uncertainties due to the use of average level-density parameters obtained from neighboring nuclei. Taking these errors into consideration, the magnitude of the calculated cross sections is in reasonable agreement with the measurements, especially at 10.5 MeV.

For both sets of optical parameters, the shape

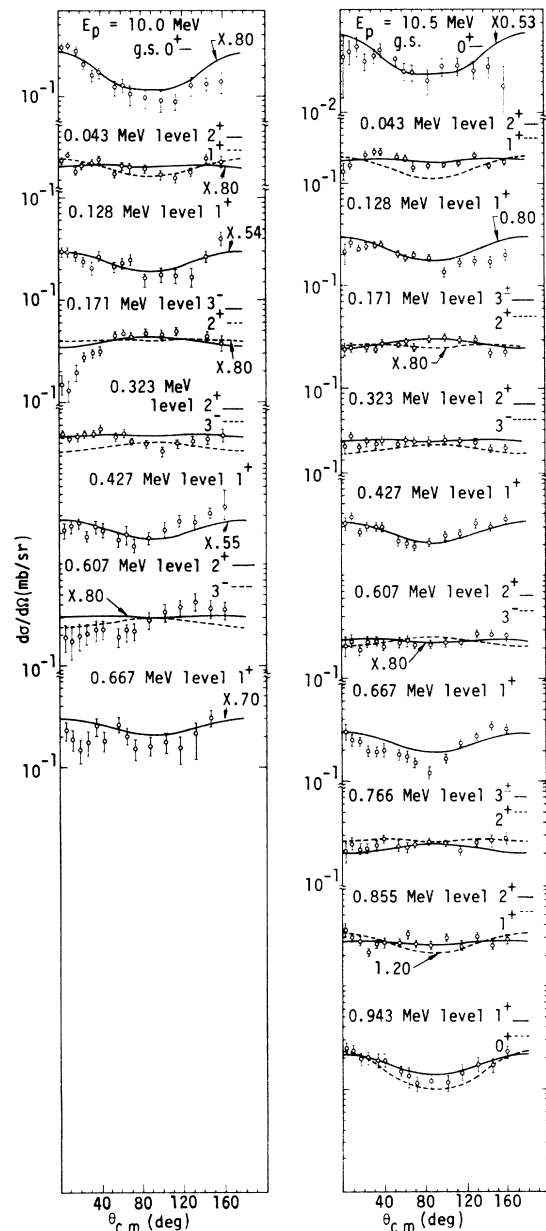


FIG. 7. Measured differential neutron cross sections from the  $^{64}\text{Zn}(p, n)^{64}\text{Ga}$  reaction at 10.0 and 10.5 MeV. The solid curves are the Hauser-Feshbach calculations for the most probable value of  $J$ . The dashed lines correspond to the second most probable choice of  $J$ .

of the calculated angular distributions is very similar for the same  $J$  value. In Fig. 7 are shown the measured differential neutron cross sections and those calculated with Becchetti and Greenlees parameters. The calculations have been normalized to the measured angular distributions; the normalization factor is shown beside each curve. For those levels whose spin is assumed to be known the solid line represents the calculated cross section for the assumed  $J$  value. The spin of the ground state has been reported<sup>20</sup> to be  $0^+$  and the spins of the 128-, 427-, and 667-keV levels are inferred to be  $J=1^+$  from  $\beta$  decay systematics of  $^{64}\text{Ge}$  to these levels in  $^{64}\text{Ga}$ . For those levels where the spin is unknown the solid line represents the calculated cross section with the most probable value of  $J$  as inferred from the  $\gamma$ -cascade information, the dashed line being the second most probable choice, with exception of the 323-keV level which will be discussed later. The agreement in the shape of the angular distributions for the measured and calculated differential cross sections is fairly good for those levels where the  $J$  values are assumed to be known.

The  $\gamma$  rays and their intensities obtained from the measurements of the  $^{64}\text{Zn}(p, n\gamma)^{64}\text{Ga}$  reaction

TABLE III.  $\gamma$ -ray energies for the  $^{64}\text{Zn}(p, n\gamma)^{64}\text{Ga}$  reaction, the proton energies at which the  $\gamma$  rays were first observed, and their cross sections at 10 MeV.

$E_\gamma$ (keV)	$E_p$ (MeV)	$\sigma$ (mb) at 10 MeV $\pm 20\%$
$42.9 \pm 0.10$	8.14	16.5
$85.2 \pm 0.10$	8.18	43.8
$128.1 \pm 0.10$	8.23	242.
$152.0 \pm 0.10$	8.43	7.34
$227.2 \pm 0.10$	8.86	3.59 <sup>a</sup>
$280.0 \pm 0.10$	8.45	49.3
$290.9 \pm 0.10$	8.94	15.9 <sup>a</sup>
$322.9 \pm 0.10$	8.56	14.9
$363.6 \pm 0.16$	8.69	14.4
$367.1 \pm 0.12$	8.72	17.7
$384.6 \pm 0.19$	8.68	10.6
$421.0 \pm 0.50$	8.78	18.1 <sup>a</sup>
$422.6 \pm 0.20$	8.85	19.8 <sup>a</sup>
$427.0 \pm 0.06$	8.50	35.2
$434.2 \pm 0.20$	8.95	9.72
$491.7 \pm 0.12$	8.68	20.1
$495.1 \pm 0.14$	8.72	29.3
$541.1 \pm 0.15$	8.70	19.6 <sup>a</sup>
$550.4 \pm 1.0$	9.53	5.44 <sup>a</sup>
$584.3 \pm 0.16$	9.15	11.1
$663.9 \pm 0.16$	9.20	18.7 <sup>a</sup>
$666.9 \pm 0.20$	8.97	29.9 <sup>a</sup>

<sup>a</sup> These cross sections were calculated as  $4\pi d\sigma/d\Omega$  ( $90^\circ$ ), the rest were obtained from the Legendre fits to the angular distributions for the  $\gamma$  rays.



at 10 MeV are given in Table III. The accuracy for some of the listed cross sections is 20% at best since some of them were obtained from the measured cross sections at  $90^\circ$  only, and the angular distributions of the  $\gamma$  rays, although not shown in this paper, were not always isotropic. For this reason, the error for those cross sections calculated as  $\sigma = 4\pi d\sigma/d\Omega(90^\circ)$  can be as large as 20 to 30%.  $\gamma$  transition threshold energies were obtained by measuring the excitation function for the reaction between 8 and 10.0 MeV. Between 8.000 and 8.300 MeV, the excitation functions were measured in 20-keV steps; above 8.300 MeV, in 50-keV steps. They were useful in determining the most probable  $\gamma$  cascades between the levels in  $^{64}\text{Ga}$ . In Table III are listed the proton energies at which the  $\gamma$  rays were first observed. To determine the  $Q$  value for the  $^{64}\text{Zn}(p, n)^{64}\text{Ga}$  ground-state reaction, the thresholds for the 42.89-, 85.24-, 128.12-, and 427.02-keV  $\gamma$  rays were used and a value of  $-7.968 \pm 0.020$  MeV was obtained. The error quoted here corresponds to the uncertainty in tandem energy which was determined by measuring the threshold of the  $(p, n)$  reaction on  $^{27}\text{Al}$  plus the error in the de-

termination of the thresholds.

From the combined information of the neutron levels and the  $\gamma$  rays observed, the level scheme of  $^{64}\text{Ga}$  shown in Fig. 8 was constructed. The energies assigned to the levels in  $^{64}\text{Ga}$  were obtained from the  $\gamma$ -ray information, when available. Using the energies inferred from the neutron spectra alone, some of the  $\gamma$  rays can be assigned to different positions in the level scheme. The evidence regarding the 42- and 128-keV radiations is discussed below.

42.89-keV  $\gamma$  ray

This  $\gamma$  ray results from the decay of the first excited state to the g.s. in  $^{64}\text{Ga}$ . It could also proceed from the decay of the 170.9-keV level to the 128.1-keV level. This possibility was discarded because of the evidence inferred from the timing measurements. In Fig. 6 it is shown that the 42.89-keV  $\gamma$  ray appears only in the delayed spectrum and that there is no evidence of a prompt component. The absence of this last, together with the fact that the 128.1-keV  $\gamma$  ray, which also can proceed from the 170.9-keV level, shows only

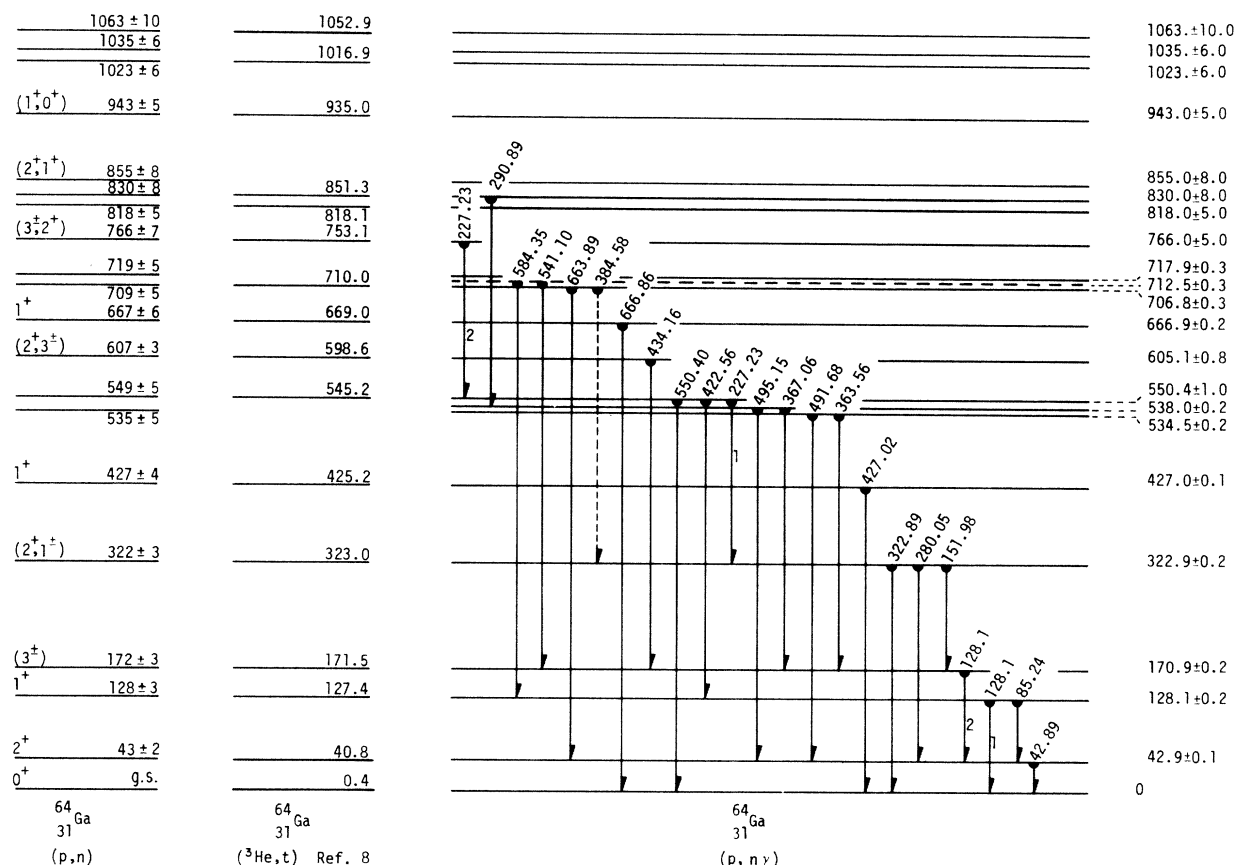


FIG. 8. Level scheme of  $^{64}\text{Ga}$  constructed from the measured  $(p, n)$  and  $(p, n\gamma)$  spectra.

in the prompt spectrum (Fig. 6), implies that the lifetime of the 170.9-keV level is short compared to the lifetime of the 42.89-keV level. Consequently, a delayed 42.89-keV  $\gamma$  ray can only proceed from the first excited level. The long lifetime ( $T_{1/2} > 1000$  nsec) measured for the 42.89-keV  $\gamma$  ray is consistent with an  $E2$  transition; this assumption is confirmed by the consideration of the internal conversion coefficient inferred from balancing the formation and decay of the level. The internal conversion coefficients  $\alpha$  are 0.78, 0.73, 16.0, and 17.2 for  $E1$ ,  $M1$ ,  $E2$ , and  $M2$  transitions, respectively.<sup>21</sup> The quantity  $\alpha$  is defined by the expression<sup>22</sup>:

$$\bar{T}(a, b) = (1 + \alpha)T(a, b), \quad (2)$$

where  $\bar{T}(a, b)$  is the total transition probability from a nuclear state  $a$  to a state  $b$  and  $T(a, b)$  is the  $\gamma$ -transition probability between the states. The observed  $\gamma$ -decay cross section  $\sigma_{\text{decay}}$  is then related to the sum of the formation cross sections  $\sigma_{\text{form}}$  by

$$\sigma_{\text{form}} = (1 + \alpha)\sigma_{\text{decay}}. \quad (3)$$

From the level scheme shown in Fig. 8

$$\begin{aligned} \sigma_{\text{form}} = & \sigma_{\gamma}(85.24) + \sigma_{\gamma}(128.1_2) + \sigma_{\gamma}(280.05) \\ & + \sigma_{\gamma}(491.68) + \sigma_{\gamma}(495.15) + \sigma_{\gamma}(663.89) + \sigma_n(n_1). \end{aligned} \quad (4)$$

From the values of the cross sections at  $E_p = 10$  MeV listed in Tables I and II

$$\sigma_{\text{form}}(42) = 17.73 \pm 2.65 \text{ mb} + \sigma_{\gamma}(128.1_2), \quad (5)$$

$$\sigma_{\text{decay}}(42) = 1.31 \pm 0.26. \quad (6)$$

Substituting these values in Eq. (3) one obtains a value for the internal conversion coefficient  $\alpha \geq 12.5$ . This is a lower limit since any cross section for the 128.1<sub>2</sub> transition and any other unobserved transitions will increase this value, bringing it in better agreement with the value  $\alpha = 16$  for an  $E2$  transition. Multipolarities greater than 2 have values of  $\alpha$  that would render the 42-keV  $\gamma$  ray unobservable. The  $J$  value for the 42.9-keV level is therefore 2. If  $J^\pi = 2^+$  and  $\alpha = 16$ , one can calculate an upper limit for the contribution from the 128.1<sub>2</sub> assuming that no other transitions populated this level. The cross section is  $\leq 4.59 \pm 4.7$  mb. The parity cannot be firmly established from the present work, but one expects only low-lying positive parity levels in this mass region.

#### 128.1-keV $\gamma$ rays

The 128.1-keV  $\gamma$  ray can proceed from the decay of the 128.1-keV level to the g.s. as well as from the decay of the 170.9-keV level to the 42.9-keV

level. Even with the high resolution of the Si(Li) detector it was impossible to resolve two peaks for this  $\gamma$  ray, which suggests that if both decay modes contribute to the measured intensity in roughly equal amounts, their energy separation must be less than 1 keV. The total cross section measured for the 128-keV radiation was  $19.3 \pm 3.9$  mb at 10 MeV. In addition to the lower limit on the cross section for the 170.9–42.9 keV transition discussed above, the data allow three other statements about the relative intensities of the two components in the 128-keV line. By balancing formation and decay for the 128-keV level, we can conclude that  $\sigma_{128_1} \geq 1.29 \pm 0.97$  mb. Similarly, by balancing formation and decay for the 171-keV level, we find  $\sigma_{128_2} \geq 10.3 \pm 1.2$  mb. In both of these cases only the lower limits are obtainable because of the possibility that some  $\gamma$  rays feeding the level have been missed. Another lower limit for  $\sigma_{128_2}$  is available from the excitation function for the 85- and 128-keV  $\gamma$  rays. The ratio of cross sections  $\sigma_{\gamma}(128)/\sigma_{\gamma}(85)$  increases from  $2.18 \pm 0.31$  at  $E_p = 8.3$  MeV to  $7.23 \pm 0.40$  at  $E_p = 10$  MeV. Using the fact that the branching ratio  $\sigma(128_1)/\sigma(85)$  must be independent of energy then leads to the relation  $\sigma_{128_2} \geq 11.7 \pm 4.3$  mb. From the various limits it seems reasonable to conclude only that the two 128-keV  $\gamma$  rays are present in roughly equal amounts at  $E_p = 10$  MeV. The short lifetime ( $\leq 3$  nsec) ascribed to the 171–43 keV transition suggests that these levels are connected by a dipole transition; the choices for the spin of the 171-keV level are then 1, 2, or 3. A  $3^+$  assignment for the 171-keV level is consistent with the absence of a measurable 171–128(1<sup>+</sup>) transition, although this transition could also be hindered by an unusually small dipole matrix element even if the spin were 1 or 2. Furthermore, the absence of a 171-keV transition to the g.s. strengthens the assumption of a  $J$  assignment  $>1$  for this level.

#### CONCLUSION

As a result of these measurements, the level scheme of <sup>64</sup>Ga has been obtained up to 1.290-MeV excitation energy. A total of 20 levels were determined; from them, only the 42.9-, 128.1-, 427-, and 666.9-keV levels had been reported by previous experiments.<sup>1, 7, 13</sup> Figure 8 summarizes these results. The assignment of  $J^\pi$  to some of the levels is not conclusive and they are shown in parentheses. They were obtained from a comparison of the measured differential neutron cross section to the predictions of a Hauser-Feshbach calculation as well as the results of the  $\gamma$ -decay studies. The first value in the parentheses indicates only the most probable value of  $J^\pi$  for the

level. For the 128.1-, 427.0-, and 666.9-keV levels, where the  $1^+$  assignment has been obtained from measurements of the  $\beta$  decay of  $^{64}\text{Ge}$ , the present calculations supported these assignments. The half-life measurements of the 42.89-, 128.1-, and 85.24-keV  $\gamma$  rays resulted in a  $2^+$  assignment for the 42.89-keV level and confirmed the  $1^+$  assignment for the 128.1-keV level. The 170.9-keV level has been assigned a  $J^\pi = 3^+$  but these measurements do not exclude a value of  $2^+$ . These values of  $J^\pi$  were consistent with those obtained from the angular distributions of the neutrons from these levels. For the 323-keV level, calculations of the neutron angular distribution were made with spins 2 and 3. The assignment of 3 is very unlikely because the octupole decay of this level to the ground state would then compete favorably with dipole decays to higher

states. Moreover, while a spin 2 assignment fits the neutron data well at 10.5 MeV, the 10-MeV data would be fitted better by spin 1. We conclude that the most likely assignments for the 323-keV level are  $2^+$  or  $1^+$ .

#### ACKNOWLEDGMENTS

The authors would like to thank Dr. J. D. Anderson for his valuable suggestions in relation to the neutron measurements, Dr. S. M. Grimes for performing the Hauser-Feshbach calculations, T. S. Whitney for his effective help with the electronics, R. Derr for loaning us a Si(Li) detector, and Dr. S. M. Austin, Dr. C. N. Davids, Dr. N. S. P. King, and Dr. R. G. H. Robertson for exchange of information prior to the publication of their results.

\*Work performed under the auspices of the U. S. Atomic Energy Commission.

<sup>1</sup>R. G. H. Robertson and S. M. Austin, *Phys. Rev. Lett.* **29**, 130 (1972).

<sup>2</sup>C. N. Davids and D. R. Goosman, *Phys. Rev. C* **7**, 122 (1973).

<sup>3</sup>G. T. Garvey, W. J. Gerace, R. L. Jaffe, I. Talmi, and I. Kelson, *Rev. Mod. Phys.* **41**, 51 (1969).

<sup>4</sup>W. D. Arnett, J. W. Truran, and S. E. Woosley, *Astrophys. J.* **165**, 87 (1971).

<sup>5</sup>W. Hauser and H. Feshbach, *Phys. Rev.* **87**, 366 (1952).

<sup>6</sup>A. H. Wapstra and N. B. Gove, *Nucl. Data A9* (Nos. 4-5), 315 (1971).

<sup>7</sup>C. N. Davids, D. L. Matthews, and D. P. Whitmire, *Bull. Am. Phys. Soc.* **17**, 71 (1972).

<sup>8</sup>R. G. H. Robertson, Michigan State University Report No. MSUCL-106, 1974 (unpublished).

<sup>9</sup>J. D. Anderson and C. Wong, *Nucl. Instrum. Methods* **15**, 178 (1962); B. D. Walker, J. D. Anderson, J. W. McClure, and C. Wong, *ibid.* **29**, 333 (1964).

<sup>10</sup>F. S. Goulding, D. A. Landis, and R. H. Pehl, Lawrence Berkeley Laboratory Report No. UCRL-17560, 1967 (unpublished).

<sup>11</sup>D. C. Camp and G. L. Meredith, *Nucl. Phys.* **A166**, 349 (1971).

<sup>12</sup>D. A. Landis, C. F. Jones, B. V. Jarrett, A. Jue, and S. D. Wright, Lawrence Berkeley Laboratory Report No. UBL-540, 1972 (unpublished).

<sup>13</sup>N. S. P. King, J. E. Draper, R. J. McDonald, *Bull. Am. Phys. Soc.* **17**, 908 (1972).

<sup>14</sup>F. Bjorklund and S. Fernbach, *Phys. Rev.* **109**, 1295 (1958).

<sup>15</sup>F. G. Perey, *Phys. Rev.* **131**, 745 (1963).

<sup>16</sup>P. E. Hodgson, *Annu. Rev. Nucl. Sci.* **17**, 1 (1967).

<sup>17</sup>F. D. Becchetti, Jr., and G. W. Greenlees, *Phys. Rev.* **182**, 1190 (1969).

<sup>18</sup>H. Verheul, *Nucl. Data B2* (No. 3), 71 (1967),  $A=64$ .

<sup>19</sup>A. Gilbert and A. G. W. Cameron, *Can. J. Phys.* **43**, 144 (1965).

<sup>20</sup>L. G. Mann, K. G. Tirsell, and S. D. Bloom, *Nucl. Phys.* **A97**, 425 (1967).

<sup>21</sup>R. S. Hager and E. C. Seltzer, *Nucl. Data A4* (No. 1), 17 (1968).

<sup>22</sup>J. M. Blatt and V. F. Weisskopf, *Theoretical Nuclear Physics* (Wiley, New York, 1952), p. 614.